

Energy spectrum of bottom- and charmed-flavored mesons from polarized top quark decay $t(\uparrow) \rightarrow W^+ + B/D + X$ at $\mathcal{O}(\alpha_s)$

S. Mohammad Moosavi Nejad*

Faculty of Physics, Yazd University, P.O. Box 89195-741, Yazd, Iran
 School of Particles and Accelerators, Institute for Research in Fundamental Sciences (IPM),
 P.O.Box 19395-5531, Tehran, Iran

(Received 2 October 2013; published 14 November 2013)

We consider the decay of a polarized top quark into a stable W^+ boson and charmed-flavored (D) or bottom-flavored (B) hadrons via $t(\uparrow) \rightarrow W^+ + D/B + X$. We study the angular distribution of the scaled energy of B/D hadrons at next-to-leading order, considering the contribution of bottom and gluon fragmentations into the heavy mesons B and D. To obtain the energy spectrum of B/D hadrons, we present our analytical expressions for the parton-level differential decay widths of $t(\uparrow) \rightarrow b + W^+ (+g)$ at next-to-leading order. A comparison of our predictions with data at the LHC enables us to test the universality and scaling violations of the B- and D-hadron fragmentation functions. These can also be used to determine the polarization states of top quarks, and since the energy distributions depend on the ratio m_W/m_t , we advocate the use of such angular decay measurements for the determination of the top quark's mass.

DOI: [10.1103/PhysRevD.88.094011](https://doi.org/10.1103/PhysRevD.88.094011)

PACS numbers: 14.65.Ha, 12.38.Bx, 13.88.+e, 14.40.Lb

I. INTRODUCTION

The top quark is the heaviest particle of the Standard Model (SM) of elementary particle physics, and its short lifetime implies that it decays before hadronization takes place; therefore, it retains its full polarization content when it decays. This allows one to study the top-spin state using the angular distributions of its decay products. Highly polarized top quarks become available at hadron colliders through single top production processes, which occur at the 33% level of the $t\bar{t}$ pair production rate [1]. Near-maximal and -minimal values of top-quark polarization at a linear e^+e^- collider can be achieved in $t\bar{t}$ production by tuning the longitudinal polarization of the beam polarization [2] so that a polarized linear e^+e^- collider may be viewed as a copious source of close to zero and close to 100% polarized top quarks. A first study of polarization in $t\bar{t}$ events was performed by the *D0* collaboration [3], which showed good agreement between the SM prediction and data.

The top-quark total width, Γ_t , is proportional to the third power of its mass and is much larger than the typical QCD scale Λ_{QCD} . Therefore, it enables us to treat the top quark almost as a free particle and to apply perturbative methods to evaluate the quantum corrections to its decay process.

The LHC is a formidable top factory that is designed to produce about 90 million top quark pairs per year of running at design c.m. energy $\sqrt{S} = 14$ TeV and design luminosity $10^{34} \text{ cm}^{-2} \text{ s}^{-1}$ in each of the four experiments [4]. This will allow one to specify the properties of the top quark, such as its total decay width Γ_t , mass m_t , and branching fractions to high accuracy. The theoretical aspects of top quark physics at the LHC are summarized in Ref. [5].

Because of the element $|V_{tb}| = 0.999152$ of the Cabibbo-Kobayashi-Maskawa [6] quark mixing matrix, top quarks almost exclusively decay to bottom quarks via $t \rightarrow bW^+$, followed by bottom-quark hadronization, $b \rightarrow H_b + X$, before b quarks decay. Here, H_b stands for the observed final-state hadron fragmented from the b quark so that its production process is regarded as the nonperturbative aspect of H_b -hadron formation from top decays. Of particular interest is the distribution in the scaled H_b -hadron energy x_H in the top-quark rest frame as reliably as possible. In Ref. [7], we calculated the doubly differential distribution $d^2\Gamma/(dx_B d\cos\theta)$ of the partial width of the decay $t \rightarrow bW^+ \rightarrow Be^+\nu_e + X$, where θ is the decay angle of the positron in the W-boson rest frame and x_B is the scaled energy of bottom-flavored hadrons B. In Ref. [8], we also evaluated the first-order QCD corrections to the energy distribution of B hadrons from the decay of an unpolarized top quark into a charged-Higgs boson via $t \rightarrow bH^+ \rightarrow BH^+ + X$ in the theories beyond the SM with an extended Higgs sector. In Ref. [9], it is mentioned that a clear separation between the decay modes $t \rightarrow bW^+$ and $t \rightarrow bH^+$ can be achieved in both the $t\bar{t}X$ pair production and the $t/\bar{t}X$ single top production at the LHC.

Since bottom quarks hadronize before they decay, the particular purpose of this paper is the evaluation of the next-to-leading-order (NLO) QCD corrections to the energy distribution of charmed-flavored (D) and bottom-flavored (B) hadrons from the decay of a polarized top quark into a bottom quark via $t(\uparrow) \rightarrow W^+ + b(\rightarrow B/D + X)$, where D stands for one of the mesons D^0 , D^+ , or D^{*+} . These measurements will be important to deepen our understanding of the nonperturbative aspects of D- and B-meson formation, which are described by realistic and nonperturbative fragmentation functions (FFs). The $b \rightarrow B$

*mmoosavi@yazduni.ac.ir

FF is obtained through a global fit to e^+e^- data from CERN LEP1 and SLAC SLC in Ref. [10], and the $b \rightarrow D^0/D^+/D^{*+}$ FFs are determined in Ref. [11] by fitting the e^+e^- experimental data from the BELLE, CLEO, OPAL, and ALEPH collaborations. As was demonstrated in Ref. [7], the finite- m_b corrections are rather small, and thus to study the distributions in the heavy meson scaled energy (x_B for B mesons and x_D for D mesons), we employ the massless scheme or zero-mass variable-flavor-number (ZM-VFN) scheme [12] in the top-quark rest frame, where the zero-mass parton approximation is also applied to the bottom quark. The nonzero value of the b-quark mass only enters through the initial condition of the nonperturbative FF.

This paper is structured as follows. In Sec. II, we introduce the angular structure of differential decay width by defining the technical details of our calculations. In Sec. III, our analytic results for the $\mathcal{O}(\alpha_s)$ QCD corrections to the angular distributions of partial decay rates are presented. In Sec. IV, we present our numerical analysis. In Sec. V, our conclusions are summarized.

II. ANGULAR DECAY DISTRIBUTION

In this section, we explain the $\mathcal{O}(\alpha_s)$ radiative corrections to the partial decay rate $t(\uparrow) \rightarrow W^+ + b$. The dynamics of the current-induced $t \rightarrow b$ transition is depicted in the hadron tensor $H^{\mu\nu}$, which is introduced by

$$H^{\mu\nu} = (2\pi)^3 \sum_{X_b} \int d\Pi_f \delta^4(p_t - p_W - p_{X_b}) \times \frac{1}{2m_t} \langle t(p_t, s_t) | J^{\nu+} | X_b \rangle \langle X_b | J^\mu | t(p_t, s_t) \rangle, \quad (1)$$

where $d\Pi_f$ refers to the Lorentz-invariant phase space factor. In the SM, the weak current is given by $J^\mu \propto \bar{q}_b \gamma^\mu (1 - \gamma_5) q_t$. Since we are not summing over the top-quark spin, the hadron tensor $H^{\mu\nu}$ also depends on the top spin s_t . In this work, we shall be concerned only with two types of intermediate states in Eq. (1), i.e., $|X_b\rangle = |b\rangle$ for the Born term and $\mathcal{O}(\alpha_s)$ one-loop contributions and $|X_b\rangle = |b + g\rangle$ for the $\mathcal{O}(\alpha_s)$ tree graph contribution. The decay $t(\uparrow) \rightarrow W^+ + b$ is analyzed in the rest frame of the top quark (Fig. 1), in which the 3-momentum of the b quark points to the direction of the positive z axis.

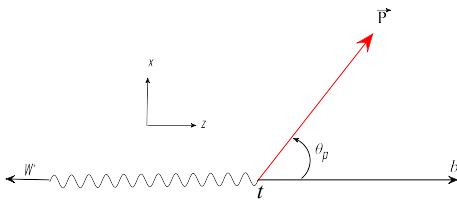


FIG. 1 (color online). Definition of the polar angle θ_p in the top-quark rest frame. \vec{P} is the polarization vector of the top quark.

The polar angle θ_p is defined as the angle between the top-quark polarization vector \vec{P} and the z axis. We shall closely follow the notation of Ref. [7], in which we discussed the $\mathcal{O}(\alpha_s)$ radiative corrections to the partial decay rate of unpolarized top quarks.

The angular distribution of the top quark differential decay width $d\Gamma/dx$ is given by the simple expression to clarify the correlations between the top quark decay products and the top spin,

$$\frac{d^2\Gamma}{dx_b d \cos \theta_p} = \frac{1}{2} \left(\frac{d\Gamma^{\text{unpol}}}{dx_b} + P \frac{d\Gamma^{\text{pol}}}{dx_b} \cos \theta_p \right), \quad (2)$$

where we have defined the b-quark scaled energy as

$$x_b = \frac{2E_b}{m_t(1 - \omega)}, \quad (3)$$

with ω being $\omega = m_W^2/m_t^2$. Neglecting the b-quark mass, one has $0 \leq x_b \leq 1$. In Eq. (2), P is the magnitude of the top-quark polarization with $0 \leq P \leq 1$ such that $P = 0$ corresponds to an unpolarized top quark and $P = 1$ corresponds to 100% top-quark polarization. $d\Gamma^{\text{unpol}}/dx_b$ and $d\Gamma^{\text{pol}}/dx_b$ stand for the unpolarized and polarized differential rates, respectively. In the following, we discuss the technical details of our calculation for the $\mathcal{O}(\alpha_s)$ radiative corrections to the tree-level decay rate of $t(\uparrow) \rightarrow b + W^+$ using dimensional regularization.

A. BORN TERM RESULTS

The Born term tensor is calculated by squaring the Born term amplitude, which is given by

$$M_0 = \frac{-eV_{tb}}{2\sqrt{2} \sin \theta_W} \bar{u}(p_b, s_b) \gamma^\mu (1 - \gamma_5) u(p_t, s_t) \epsilon_\mu^*(p_W, \lambda), \quad (4)$$

where ϵ^μ stands for the W-boson polarization vector, the angle θ_W is the weak mixing angle, and we take $\sin^2 \theta_W = 0.23124$ [13]; s and p stand for the spin and 4-momentum of particles, respectively. The squared Born amplitude is expressed as

$$|M_0|^2 = \sum_{s_b, s_W} M_0 M_0^\dagger = \frac{e^2}{2\sin^2 \theta_W} \left[p_b \cdot p_t - m_t p_b \cdot s_t + \frac{2}{m_W^2} (p_b \cdot p_W)(p_t \cdot p_W) - 2 \frac{m_t}{m_W^2} (p_b \cdot p_W)(p_W \cdot s_t) \right], \quad (5)$$

where we replaced $\sum_{s_t} u(p_t, s_t) \bar{u}(p_t, s_t) = (\not{p}_t + m_t)$ in the unpolarized Dirac string by $u(p_t, s_t) \bar{u}(p_t, s_t) = 1/2(1 - \gamma_5 \delta_t)(\not{p}_t + m_t)$ in the polarized state.

Considering Fig. 1, we parametrize the 4-momentum and the polarization vector in the top rest frame as

$$p_b = (E_b, 0, 0, E_b), \quad p_W = (E_W, 0, 0, -E_b), \quad (6)$$

$$s_t = P(0, \sin \theta_p \cos \phi_p, \sin \theta_p \sin \phi_p, \cos \theta_p),$$

where the parameter P is the degree of polarization. Therefore, the leading-order (LO) amplitude squared reads

$$|M_0|^2 = \frac{\pi\alpha}{\sin^2 \theta_W} \frac{1-\omega}{\omega} m_t^2 [1 + 2\omega + P(1-2\omega)\cos \theta_p], \quad (7)$$

Here, $\pi\alpha/\sin^2 \theta_W$ is related to the Fermi constant G_F as $\sqrt{2}m_W^2 G_F$.

The decay rate of a particle with a mass m and momentum p into a given final state of particles (p_1, p_2, \dots, p_n) is

$$d\Gamma = \frac{1}{2m} \prod_{i=1}^n \frac{d^3 p_i}{(2\pi)^3} \frac{1}{2E_i} (2\pi)^4 \delta^4\left(p - \sum_{i=1}^n p_i\right) |M(m \rightarrow \{p_i\})|^2,$$

$$= \frac{1}{2m} \frac{1}{(2\pi)^{3n-4}} dR_n(p, p_1, p_2, \dots, p_n) |M(m \rightarrow \{p_i\})|^2, \quad (8)$$

where in the two-body phase space (e.g., $t \rightarrow b + W^+$), using the relation

$$\int \frac{d^3 \vec{p}}{2E} = \int d^4 p \delta(p^2 - m^2) \Theta(E), \quad (9)$$

one has

$$dR_2(p_t, p_b, p_W) = \frac{1-\omega}{8} (2\pi d \cos \theta_p). \quad (10)$$

Substituting Eqs. (7) and (10) into Eq. (8), one has

$$\frac{d\Gamma_0}{d \cos \theta_p} = \frac{1}{2} \{\Gamma_0^{\text{unpol}} + P \Gamma_0^{\text{pol}} \cos \theta_p\}, \quad (11)$$

where the polarized and unpolarized Born term rates read

$$\Gamma_0^{\text{unpol}} = \frac{m_t^3 G_F}{8\sqrt{2}\pi} (1+2\omega)(1-\omega)^2 \quad (12)$$

and

$$\Gamma_0^{\text{pol}} = \frac{m_t^3 G_F}{8\sqrt{2}\pi} (1-2\omega)(1-\omega)^2. \quad (13)$$

To check our results, we note that the LO expression for the unpolarized top decay rate (12) is in agreement with Eqs. (23) and (24) of Refs. [14,15], respectively, and the polarized Born rate (13) is in consistency with Eqs. (24) and (13) of Refs. [15,16], respectively, by the replacement $\omega \rightarrow x^2$.

The polarization asymmetry α_W is defined by $\alpha_W = \Gamma_0^{\text{pol}}/\Gamma_0^{\text{unpol}}$, which is simplified to $\alpha_W = (1-2\omega)/(1+2\omega) = 0.396$ if we set $m_W = 80.399$ GeV and $m_t = 172.9$ GeV [17].

B. ONE-LOOP CONTRIBUTION

The virtual one-loop contributions to the fermionic vector-axial (V-A) transitions have a long history. Since at the one-loop level QED and QCD have the same structure, then the history even dates back to QED times. In this section, we will investigate the one-loop corrections and describe the method applied to extract the singularities at zero-mass scheme. In the ZM-VFN scheme, where $m_b = 0$ is set right from the start, both the soft and collinear singularities are regularized by dimensional regularization in $D = 4 - 2\epsilon$ space-time dimensions to become single poles in ϵ ($0 < \epsilon \leq 1$). These singularities are subtracted at factorization scale μ_F and absorbed into the bare FFs according to the modified minimal-subtraction ($\overline{\text{MS}}$) scheme. This renormalizes the FFs and creates in $d\Gamma/dx_b$ finite terms including the term $\alpha_S \ln(\mu_F^2/m_t^2)$, which are rendered perturbatively small by choosing $\mu_F = \mathcal{O}(m_t)$.

The virtual contributions exhibit both the IR and UV singularities, which are regularized in D dimensions. To evaluate the one-loop contributions to $t(\uparrow) \rightarrow b + W^+$, we consider the Feynman diagrams drawn in Fig. 2. The renormalized amplitude of the virtual corrections can be written as

$$M_{\text{loop}} = \frac{-e}{2\sqrt{2} \sin \theta_W} \epsilon_\mu^*(p_W) \bar{u}(p_b, s_b) \{\Lambda_\mu + \delta\Lambda_\mu\} u(p_t, s_t). \quad (14)$$

Considering Fig. 2(a), the counterterm of the vertex is given by $\delta\Lambda_\mu = (\delta Z_b/2 + \delta Z_t/2)\gamma_\mu(1-\gamma_5)$, where the wave-function renormalization constants of the top (δZ_t) and bottom (δZ_b) can be found in Ref. [8]. From Fig. 2(b), for the one-loop vertex correction, one has

$$\Lambda_\mu = \frac{C_F \alpha_S}{4i\pi^3} \int d^4 p_g \frac{\gamma^\beta (\not{p}_b + \not{p}_g) \gamma_\mu (1-\gamma_5) (\not{p}_t + m_t) \gamma_\beta}{p_g^2 (p_b + p_g)^2 (p_t^2 - m_t^2)}, \quad (15)$$

where $C_F = 4/3$ stands for the color factor and p_g refers to the gluon 4-momentum. The integral (15) is both IR- and UV-divergent, and we use dimensional regularization to extract singularities taking the replacement

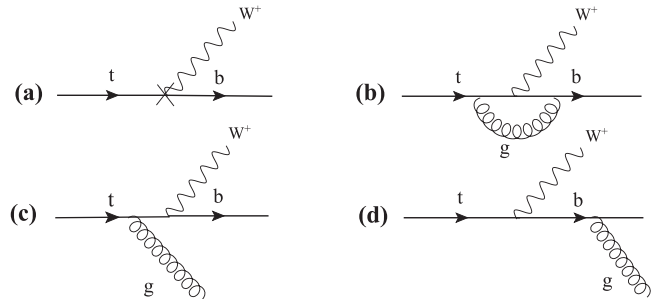


FIG. 2. Virtual (a, b) and real gluon (c, d) contributions to $t(\uparrow) \rightarrow b + W^+$ at NLO.

$$\int \frac{d^4 p_g}{(2\pi)^4} \rightarrow \mu^{4-D} \int \frac{d^D p_g}{(2\pi)^D}. \quad (16)$$

At $\mathcal{O}(\alpha_s)$, the full amplitude is the sum of the amplitudes of the Born term, virtual one-loop, and the real contributions

$$M = M_0 + M_{\text{loop}} + M_{\text{real}}. \quad (17)$$

Squaring the full amplitude, we have

$$|M|^2 = |M_0|^2 + |M_{\text{vir}}|^2 + |M_{\text{real}}|^2 + \mathcal{O}(\alpha_s^2), \quad (18)$$

where $|M_{\text{vir}}|^2 = 2M_0^\dagger M_{\text{loop}}$ and $|M_{\text{real}}|^2 = M_{\text{real}}^\dagger M_{\text{real}}$. Considering Eqs. (8) and (10), the virtual corrections to the doubly differential decay rate are then given by

$$\frac{d^2 \Gamma_{\text{vir}}}{dx_b d \cos \theta_p} = \frac{1 - \omega}{32\pi m_t} |M_{\text{vir}}|^2 \delta(1 - x_b), \quad (19)$$

where x_b is defined in Eq. (3). The one-loop vertex correction and the wave-function renormalization contain UV and IR singularities that all UV singularities are canceled after summing all virtual corrections up, whereas the IR divergences are remaining, which are now labeled by ϵ . Therefore, the virtual doubly differential distribution reads

$$\frac{d^2 \Gamma_{\text{vir}}}{dx_b d \cos \theta_p} = \frac{1}{2} \left(\frac{d\Gamma_{\text{vir}}^{\text{unpol}}}{dx_b} + P \frac{d\Gamma_{\text{vir}}^{\text{pol}}}{dx_b} \cos \theta_p \right), \quad (20)$$

where the unpolarized differential decay rate normalized to the unpolarized Born term is

$$\frac{1}{\Gamma_0^{\text{unpol}}} \frac{d\Gamma_{\text{vir}}^{\text{unpol}}}{dx_b} = \frac{C_F \alpha_S}{2\pi} \left[A - 4 \frac{1 - \omega}{1 - 4\omega^2} \ln(1 - \omega) \right] \delta(1 - x_b), \quad (21)$$

and the polarized differential width normalized to the polarized Born width reads

$$\frac{1}{\Gamma_0^{\text{pol}}} \frac{d\Gamma_{\text{vir}}^{\text{pol}}}{dx_b} = \frac{C_F \alpha_S}{2\pi} A \delta(1 - x_b), \quad (22)$$

with

$$\begin{aligned} A = & -\frac{1}{2} \left(2 \ln(1 - \omega) - \ln \frac{4\pi \mu_F^2}{m_t^2} + \gamma_E - \frac{5}{2} \right)^2 \\ & + \frac{1}{\epsilon} \left(2 \ln(1 - \omega) - \ln \frac{4\pi \mu_F^2}{m_t^2} + \gamma_E - \frac{5}{2} \right) \\ & - \frac{1 - 4\omega}{1 - 2\omega} \ln(1 - \omega) + 2 \ln \omega \ln(1 - \omega) \\ & + 2Li_2(1 - \omega) - \frac{1}{\epsilon^2} - 5 \frac{\pi^2}{12} - \frac{23}{8}. \end{aligned} \quad (23)$$

Here, $\gamma_E = 0.5772 \dots$ is the Euler constant, and the dilogarithmic function $Li_2(x)$ is defined as

$$Li_2(x) = - \int_0^x \frac{\ln(1 - z)}{z} dz. \quad (24)$$

As is seen, the one-loop contribution is purely real. This can be gotten from an inspection of the one-loop Feynman diagram, Fig. 2(b), which does not accept any nonvanishing physical two-particle cut.

C. TREE GRAPH CONTRIBUTION

The $\mathcal{O}(\alpha_s)$ real graph contribution results from the square of the real gluon emission graphs shown in Figs. 2(c) and 2(d). The real amplitude for the decay process $t(\uparrow) \rightarrow b(p_b) + W^+(p_W) + g(p_g)$ reads

$$\begin{aligned} M_{\text{real}} = & e g_s \frac{T_{ij}^n}{2\sqrt{2} \sin \theta_W} \bar{u}(p_b, s_b) \left\{ \frac{\gamma^\mu \not{p}_g \gamma^\beta - 2p_t^\beta \gamma^\mu}{2p_t \cdot p_g} \right. \\ & \left. + \frac{\gamma^\beta \not{p}_g \gamma^\mu + p_b^\beta \gamma^\mu}{2p_b \cdot p_g} \right\} (1 - \gamma_5) u(p_t, s_t) \epsilon_{\beta}^*(p_g, s_g), \end{aligned} \quad (25)$$

where g_s is the strong coupling constant, n is the color index ($n = 1, 2, 3, \dots, 8$) so $\text{Tr}(T^n T^n)/3 = C_F$, and the first and second terms in the curly brackets refer to real gluon emission from the top quark and the bottom quark, respectively. The polarization vector of the gluon is denoted by $\epsilon(p_g, s_g)$. By working in the massless scheme, the mass of the b quark is set to zero; thus, the IR divergences arise from the soft- and collinear-gluon emission. As before, to regulate the IR singularities, we work in D dimensions. In the top-quark rest frame (Fig. 3), the momenta and the polarization vector are defined as

$$\begin{aligned} p_b = & E_b(1, 0, 0, 1), & p_g = & E_g(1, \sin \theta, 0, \cos \theta), \\ s_t = & P(0, \sin \theta_p \cos \phi_p, \sin \theta_p \sin \phi_p, \cos \theta_p). \end{aligned} \quad (26)$$

Considering Eq. (8), the real differential rate in D dimensions is given by

$$\begin{aligned} d\Gamma_{\text{real}} = & \frac{1}{2m_t} \frac{\mu_F^{2(4-D)}}{(2\pi)^{2D-3}} |M_{\text{real}}|^2 \frac{d^{D-1} \vec{p}_b}{2E_b} \frac{d^{D-1} \vec{p}_W}{2E_W} \frac{d^{D-1} \vec{p}_g}{2E_g} \\ & \times \delta^D(p_t - p_b - p_g - p_W). \end{aligned} \quad (27)$$

To calculate the differential decay rate $d\Gamma_{\text{real}}/dx_b$ normalized to the Born width, we fix the momentum of the b quark and integrate over the energy of the gluon,

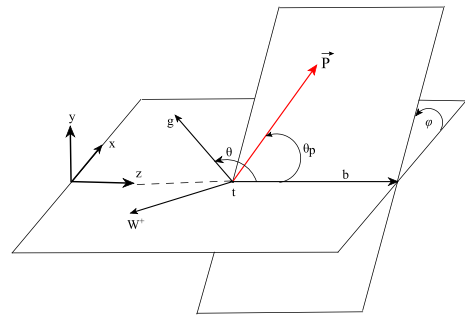


FIG. 3 (color online). Definition of the azimuthal angle ϕ and the polar angles θ and θ_p . \vec{P} is the polarization vector of the top quark.

which ranges from $E_g^{\min} = m_i(1 - \omega)(1 - x_b)/2$ to $E_g^{\max} = m_i(1 - \omega)(1 - x_b)/(2(1 - x_b(1 - \omega)))$, and to obtain the angular distribution of differential width $d^2\Gamma_{\text{real}}/(dx_b d\cos\theta_P)$, the angular integral in D dimensions is written as

$$d\Omega_b = \frac{2\pi^{\frac{D}{2}-1}}{\Gamma(\frac{D}{2}-1)} (\sin\theta_P)^{D-4} d\cos\theta_P. \quad (28)$$

In the massless scheme, the real and virtual differential widths contain the poles $\propto 1/\epsilon$ and $1/\epsilon^2$, which disappear only in the total NLO width. This requires that to get the correct finite terms in the normalized doubly differential distribution $1/\Gamma_0 \times d^2\Gamma_{\text{real}}/(dx_b d\cos\theta_P)$, the polarized and unpolarized Born widths will have to be evaluated in dimensional regularization at $\mathcal{O}(\epsilon^2)$. We find

$$\begin{aligned} \Gamma_0^{\text{unpol}} &= \frac{m_i^3 G_F}{8\sqrt{2}\pi} (1+2\omega)(1-\omega)^2 \left[1 + \epsilon F + \epsilon^2 \left[\frac{F^2}{2} + 2 \frac{(1+\omega)(1+3\omega)}{(1+2\omega)^2} - \frac{\pi^2}{4} \right] \right], \\ \Gamma_0^{\text{pol}} &= \frac{m_i^3 G_F}{8\sqrt{2}\pi} (1-2\omega)(1-\omega)^2 \left[1 + \epsilon \left[H + \frac{2\omega}{1-2\omega} \right] + \epsilon^2 \left[\frac{1}{2} \left(H + \frac{5}{2} \right)^2 - H \frac{5-14\omega}{2(1-2\omega)} - \frac{\pi^2}{12} - \frac{25}{8} \right] \right], \end{aligned} \quad (29)$$

with

$$\begin{aligned} F &= \ln \frac{4\pi\mu_F^2}{m_i^2} - 2\ln(1-\omega) - \gamma_E + 2 \frac{1+\omega}{1+2\omega}, \\ H &= \ln \frac{4\pi\mu_F^2}{m_i^2} - 2\ln \frac{1-\omega}{2} - \gamma_E. \end{aligned} \quad (30)$$

Now, the real gluon contribution is given by

$$\frac{d^2\Gamma_{\text{real}}}{dx_b d\cos\theta_P} = \frac{1}{2} \left(\frac{d\Gamma_{\text{real}}^{\text{unpol}}}{dx_b} + P \frac{d\Gamma_{\text{real}}^{\text{pol}}}{dx_b} \cos\theta_P \right), \quad (31)$$

where, by defining $T = -\ln(4\pi\mu_F^2/m_i^2) + 2\ln(1-\omega) + \gamma_E$, one has

$$\begin{aligned} \frac{1}{\Gamma_0^{\text{unpol}}} \frac{d\Gamma_{\text{real}}^{\text{unpol}}}{dx_b} &= \frac{C_F \alpha_S}{2\pi} \left\{ \delta(1-x_b) \left[\frac{1}{2} T^2 - T + \frac{1}{\epsilon^2} - \frac{2\omega}{1-\omega} \ln\omega + 2Li_2(1-\omega) - \frac{1}{\epsilon} (T-1) - \frac{\pi^2}{4} \right] + 2(1+x_b^2) \left(\frac{\ln(1-x_b)}{1-x_b} \right)_+ \right. \\ &\quad \left. + \frac{1}{(1-x_b)_+} \left[1 - 4x_b + x_b^2 + \frac{4x_b\omega(1-\omega)(1-x_b)^2}{(1+2\omega)(1-x_b(1-\omega))} + (1+x_b^2) \left(\ln \left[\frac{x_b^2(1-\omega)^2 m_i^2}{4\pi\mu_F^2} \right] + \gamma_E - \frac{1}{\epsilon} \right) \right] \right\}, \end{aligned} \quad (32)$$

and

$$\begin{aligned} \frac{1}{\Gamma_0^{\text{pol}}} \frac{d\Gamma_{\text{real}}^{\text{pol}}}{dx_b} &= \frac{C_F \alpha_S}{2\pi} \left\{ \delta(1-x_b) \left[\frac{1}{2} T^2 - T - \frac{2\omega}{1-\omega} \ln\omega + 2Li_2(1-\omega) - \frac{1}{\epsilon} (T-1) + \frac{1}{\epsilon^2} - \frac{\pi^2}{4} \right] \right. \\ &\quad \left. + 2(1+x_b^2) \left(\frac{\ln(1-x_b)}{1-x_b} \right)_+ + \frac{1}{(1-x_b)_+} \left[-1 - x_b^2 + \frac{8\omega(1-x_b)^2}{1-2\omega} + 4 \frac{x_b\omega(1-\omega)(1-x_b)^2}{(1-2\omega)(1-x_b(1-\omega))} \right. \right. \\ &\quad \left. \left. + (1+x_b^2) \left(\ln \left[\frac{x_b^2(1-\omega)^2 m_i^2}{4\pi\mu_F^2} \right] + \gamma_E - \frac{1}{\epsilon} \right) + \frac{8\omega(1-x_b)^2}{x_b(1-\omega)(1-2\omega)} \ln(1-x_b(1-\omega)) \right] \right\}. \end{aligned} \quad (33)$$

III. ANALYTIC RESULTS FOR ANGULAR DISTRIBUTION OF PARTIAL DECAY RATES

Now, we are in a situation to present our analytic results for the angular distribution of the differential decay rate by summing the Born-level (11), the virtual (20), and real gluon (31) contributions. According to the Lee–Nauenberg theorem, all singularities cancel each other after summing all contributions up, and the final

result is free of IR singularities. Therefore, the complete $\mathcal{O}(\alpha_s)$ results are

$$\frac{d^2\Gamma}{dx_b d\cos\theta_P} = \frac{1}{2} \left\{ \frac{d\Gamma_{\text{NLO}}^{\text{unpol}}}{dx_b} + P \frac{d\Gamma_{\text{NLO}}^{\text{pol}}}{dx_b} \cos\theta_P \right\}, \quad (34)$$

where we presented $d\Gamma_{\text{NLO}}^{\text{unpol}}/dx_b$ in Ref. [7] and $d\Gamma_{\text{NLO}}^{\text{pol}}/dx_b$ in the $\overline{\text{MS}}$ scheme is expressed, for the first time, as

$$\begin{aligned} \frac{1}{\Gamma_0^{\text{pol}}} \frac{d\Gamma_{\text{NLO}}^{\text{pol}}}{dx_b} &= \delta(1-x_b) + \frac{C_F \alpha_s}{2\pi} \left\{ \delta(1-x_b) \left[-\frac{3}{2} \ln \frac{\mu_F^2}{m_t^2} + 2 \frac{1-\omega}{1-2\omega} \ln(1-\omega) - 2 \frac{\omega}{1-\omega} \ln \omega - \frac{2\pi^2}{3} \right. \right. \\ &+ 2 \ln \omega \ln(1-\omega) + 4 \text{Li}_2(1-\omega) - 6 \left. \right] + 2(1+x_b^2) \left(\frac{\ln(1-x_b)}{1-x_b} \right)_+ + \frac{1}{(1-x_b)_+} \left[-1 - x_b^2 + \frac{8\omega(1-x_b)^2}{1-2\omega} \right. \\ &\left. \left. + 4 \frac{x_b \omega(1-\omega)(1-x_b)^2}{(1-2\omega)(1-x_b(1-\omega))} + (1+x_b^2) \ln \left[x_b^2(1-\omega)^2 \frac{m_t^2}{\mu_F^2} \right] + \frac{8\omega(1-x_b)^2}{x_b(1-\omega)(1-2\omega)} \ln(1-x_b(1-\omega)) \right] \right\}. \end{aligned} \quad (35)$$

Considering the plus prescription, defined as

$$\int_0^1 (g(x_b))_+ h(x_b) dx_b = \int_0^1 g(x_b) [h(x_b) - h(1)] dx_b, \quad (36)$$

and by integrating $d\Gamma_{\text{NLO}}/dx_b$ over $x_b(0 \leq x_b \leq 1)$, we have checked our polarized and unpolarized results against known results [15,18] and found agreement.

Since the observed mesons can be also produced through a fragmenting gluon, therefore, to obtain the most accurate result for the energy spectrum of the meson, we have to add the contribution of gluon fragmentation to the b quark to produce the outgoing meson. From Fig. 4, it is seen that the contribution of the gluon decreases the size of the decay rate

up to 40% at the threshold; thus, this contribution can be important at a low energy of the observed meson. Therefore, the differential decay rate $d\Gamma/dx_g$ is also required, where x_g is defined as $x_g = 2E_g/(m_t(1-\omega))$ as in Eq. (3). To obtain the doubly differential distribution $d^2\Gamma/(dx_g d\cos\theta_P)$, we integrate over the b-quark energy by fixing the gluon momentum in the phase space. The result is

$$\frac{d^2\Gamma}{dx_g d\cos\theta_P} = \frac{1}{2} \left\{ \Gamma_{\text{NLO}}^{\text{unpol}} \frac{d\Gamma_{\text{NLO}}^{\text{pol}}}{dx_g} \cos\theta_P \right\}, \quad (37)$$

where $d\Gamma_{\text{NLO}}^{\text{unpol}}/dx_g$ can be found in our previous work [7] and $d\Gamma_{\text{NLO}}^{\text{pol}}/dx_g$ is listed here:

$$\begin{aligned} \frac{1}{\Gamma_0^{\text{pol}}} \frac{d\Gamma_{\text{NLO}}^{\text{pol}}}{dx_g} &= \frac{C_F \alpha_s}{2\pi} \left\{ \frac{2}{x_g^2} \ln(1-x_g(1-\omega)) \left[\frac{(1-2x_g)^2}{1-\omega} + \frac{4x_g(1-x_g)}{1-2\omega} \right] \right. \\ &+ \frac{1}{2(1-2\omega)} \left[2(1-2\omega) + \frac{4(1+\omega)}{1-\omega} - x_g(1+6\omega) - \frac{\omega(6\omega^2+\omega+2)}{(1-\omega)(1-x_g(1-\omega))} - \frac{\omega^2(1-2\omega)}{(1-\omega)(1-x_g(1-\omega))^2} \right] \\ &\left. + \frac{1+(1-x_g)^2}{x_g} \left[2 \ln(x_g(1-x_g)) - \ln \frac{\mu_F^2}{m_t^2} - \ln(1-x_g(1-\omega)) + 2 \ln(1-\omega) \right] \right\}. \end{aligned} \quad (38)$$

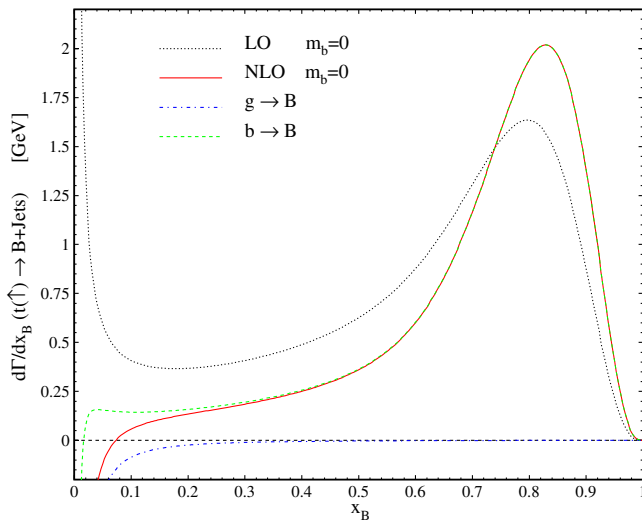


FIG. 4 (color online). $d\Gamma(t(\bar{t}) \rightarrow BW^+ + X)/dx_B$ as a function of x_B in the ZM-VFN ($m_b = 0$) scheme. The NLO result (solid line) is compared to the LO one (dotted line) and broken up into the contributions due to $b \rightarrow B$ (dashed line) and $g \rightarrow B$ (dotted-dashed line) fragmentation. We set $\mu_F = m_t$ and $\mu_{0F} = m_b$.

IV. NONPERTURBATIVE FRAGMENTATION AND HADRON LEVEL RESULTS

In this section, performing a numerical analysis, we present our phenomenological results for the energy spectrum of the heavy mesons B and D from polarized top decays and compare them with the unpolarized one in Ref. [7]. We define the normalized-energy fractions of the outgoing mesons similarly to the parton-level one in Eq. (3) as $x_B = 2E_B/(m_t(1-\omega))$ for the B meson and $x_D = 2E_D/(m_t(1-\omega))$ for the D meson. Considering the factorization theorem of the QCD-improved parton model [19], the energy distribution of a hadron can be expressed as the convolution of the parton-level spectrum with the nonperturbative fragmentation function $D_a^H(z, \mu_F)$,

$$\frac{d\Gamma}{dx_H} = \sum_{i=b,g} \frac{d\Gamma}{dx_i}(\mu_R, \mu_F) \otimes D_i^H\left(\frac{x_H}{x_i}, \mu_F\right), \quad (39)$$

where H stands for B and D mesons and the allowed x_H ranges are $2m_H/(m_t(1-\omega)) \leq x_H \leq 1$. The integral convolution appearing in Eq. (39) is defined as

$$(f \otimes g)(x) = \int_x^1 dx f(z) g\left(\frac{x}{z}\right). \quad (40)$$

In Eq. (39), μ_F and μ_R are the factorization and the renormalization scales, respectively, and one can use two different values for these scales; however, a choice often made consists of setting $\mu_R = \mu_F$, and we adopt the convention $\mu_R = \mu_F = m_t$ for our results. In Eq. (39), $d\Gamma/dx_i$ are the parton-level differential rates presented in Eqs. (34) and (37), and D_i^H are the nonperturbative FFs describing the hadronizations $b \rightarrow H$ and $g \rightarrow H$, which are process independent. Several models have been already proposed to describe the FFs. In Ref. [11], the authors calculated the FFs for D^0 , D^+ , and D^{*+} mesons by fitting the experimental data from the BELLE, CLEO, OPAL, and ALEPH collaborations in the modified minimal-subtraction ($\overline{\text{MS}}$) factorization scheme. They parametrized the z distributions of the $b \rightarrow D^0/D^+/D^{*+}$ FFs at their starting scale $\mu_0 = m_b$, as suggested by Bowler [20], as

$$D_b^D(z, \mu_0) = N z^{-(1+\gamma^2)} (1-z)^a e^{-\gamma^2/z}, \quad (41)$$

while the FF of the gluon is set to zero and this FF is evolved to higher scales using the Dokshitzer-Gribov-Lipatov-Altarelli-Parisi equations [21]. As is claimed in Ref. [11], this parametrization yields the best fit to the BELLE data [22] in a comparative analysis using the Monte Carlo event generator JETSET/PYTHIA. The values of fit parameters together with the achieved values of $\overline{\chi^2}$ are presented in Table I. From Ref. [10], we employ the $b \rightarrow B$ FF determined at NLO in the ZM-VFN approach through a global fit to e^+e^- -annihilation data taken by ALEPH [23] and OPAL [24] at CERN LEP1 and by SLD [25] at SLAC SLC. The power ansatz $D_b^B(z, \mu_0) = N z^\alpha (1-z)^\beta$ was used as the initial condition for the $b \rightarrow B$ FF at $\mu_0 = m_b$, while the gluon FF was generated via the Dokshitzer-Gribov-Lipatov-Altarelli-Parisi evolution. The fit parameters are $N = 4684.1$, $\alpha = 16.87$, and $\beta = 2.628$ with $\overline{\chi^2} = 1.495$. Following Ref. [17], we adopt the input values $G_F = 1.16637 \times 10^{-5} \text{ GeV}^{-2}$, $m_t = 172.9 \text{ GeV}$, $m_b = 4.78 \text{ GeV}$, $m_W = 80.339 \text{ GeV}$, $m_B = 5.279 \text{ GeV}$, $m_D = 1.87 \text{ GeV}$, and $\Lambda_{\overline{\text{MS}}}^{(5)} = 231 \text{ MeV}$ with $n_f = 5$ active quark flavors and adjusted such that $\alpha_s^{(5)}(m_Z = 91.18) = 0.1184$.

To study the scaled-energy (x_B and x_D) distributions of the bottom- and charmed-flavored hadrons produced

TABLE I. Values of fit parameters for $b \rightarrow D^0$, $b \rightarrow D^+$, and $b \rightarrow D^{*+}$ FFs at the starting scale $\mu_0 = m_b$ resulting from the global fit in the ZM approach together with the values of $\overline{\chi^2}$ achieved.

	N	a	γ	$\overline{\chi^2}$
D^0	80.8	5.77	1.15	4.66
D^+	163	6.93	1.40	2.21
D^{*+}	14.9	3.87	1.16	7.64

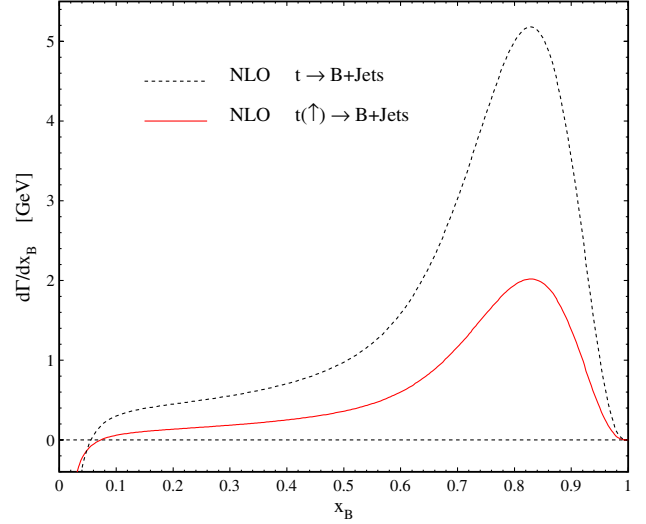


FIG. 5 (color online). $d\Gamma/dx_B$ as a function of x_B in the ZM-VFN ($m_b = 0$) scheme, considering the unpolarized (dashed line) and polarized (solid line) partial decay rates at NLO.

in the polarized top decay, we consider the quantities $d\Gamma(t(\uparrow) \rightarrow B + X)/dx_B$ and $d\Gamma(t(\uparrow) \rightarrow D + X)/dx_D$ in the ZM-VFN scheme. In Fig. 4, our prediction for the B meson is shown by studying the size of the NLO corrections, by comparing the LO (dotted line) and NLO (solid line) results, and the relative importance of the $b \rightarrow B$ (dashed line) and $g \rightarrow B$ (dotted-dashed line) fragmentation channels at NLO. We evaluated the LO result using the same NLO FFs. The $g \rightarrow B$ contribution is negative and appreciable only in the low- x_B region. For higher values of x_B , as is expected [14], the NLO result is practically exhausted by the $b \rightarrow B$ contribution. Note that the

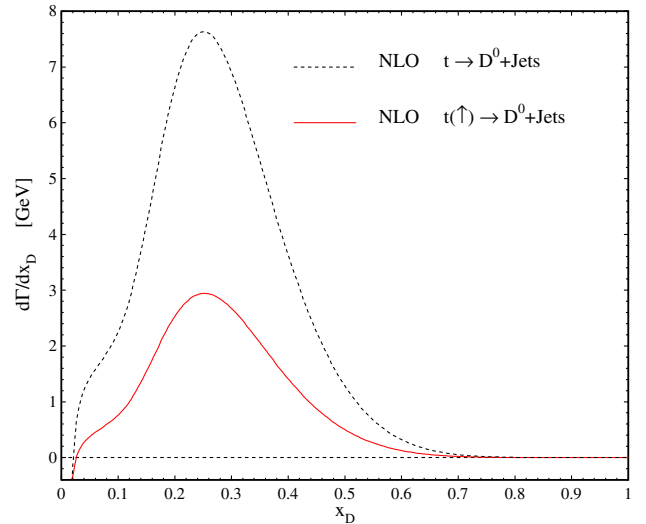


FIG. 6 (color online). x_D spectrum in top decay, with the hadronization modeled according to the Bowler model considering the unpolarized (dashed line) and polarized (solid line) decay rates at NLO. We set $\mu_F = m_t$ and $\mu_{0F} = m_b$.

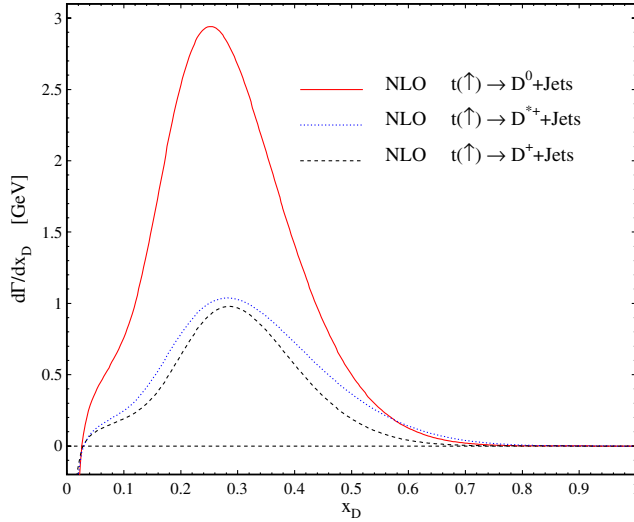


FIG. 7 (color online). $d\Gamma(t(\uparrow) \rightarrow DW^+ + X)/dx_D$ as a function of x_D at NLO for $D = D^0$ (solid line), $D = D^{*+}$ (dotted line), and $D = D^+$ (dashed line).

contribution of the gluon cannot be discriminated. It is calculated to see where it contributes to $d\Gamma/dx_B$. So, this part of the paper is of more theoretical relevance. In the scaled energy of mesons as an experimental quantity, all contributions including the b quark, gluon, and light quarks contribute. In Fig 5, the scaled-energy (x_B) distribution of B hadrons produced in unpolarized (dashed line) and polarized (solid line) top-quark decays at NLO are studied. As is seen, in the unpolarized top decay the partial decay width at the hadron level is around 38% higher than the one in the polarized top decay in the peak region. In Fig. 6, the same comparison is also done for the transition $b \rightarrow D^0$ applying the Bowler model (41) for the FFs. Figure 6 shows that the chance to produce the charmed-flavored mesons through top-quark decays in the high- x_D range ($0.7 \leq x_D$) is zero. In Fig. 7, we study the scaled-energy (x_D) distribution of charmed-flavored hadrons produced in polarized top decays as $t(\uparrow) \rightarrow D^0 + X_1$ (solid line), $t(\uparrow) \rightarrow D^{*+} + X_2$ (dotted line), and $t(\uparrow) \rightarrow D^+ + X_3$ (dashed line). Note that our results are valid just for $x_D \geq 2E_D/(m_t(1 - \omega)) = 0.028$ and $x_B \geq 0.078$.

V. CONCLUSIONS

The top-quark decays rapidly so that it has no time to hadronize and passes on its full spin information to its decay products. The CERN LHC, as a superlative top factory, allows us to study top-quark decays that within the SM are completely dominated by the mode $t \rightarrow W^+ + b$, followed by $b \rightarrow H + X$. Therefore, the distribution in the scaled H-hadron energy x_H in the top rest frame are of particular interest. In fact, the x_H distribution provides direct access to the H-hadron FFs, and its $\cos \theta_P$ distribution allows one to analyze the top-quark polarization in which the polar angle θ_P refers to the angle between the polarization vector of the top and the z axis.

In Ref. [7], we studied the scaled-energy (x_B) distribution of the B meson in unpolarized top-quark decays, and in the present work, we made our predictions for the scaled-energy (x_B, x_D) distributions of the B and D mesons in the polarized top-quark rest frame by studying the quantity $d^2\Gamma/(dx_H d\cos \theta_P)$. As was mentioned, the scaled-energy distribution of hadron enables us to deepen our knowledge of the hadronization process and to pin down the $b, g \rightarrow B/D$ FFs while the angular analysis of the polarized top decay constrain these FFs even further. Furthermore, the polarization state of top quarks can be specified from the angular distribution of the outgoing hadron energy. The universality and scaling violations of the B- and D-hadron FFs will be able to test at LHC by comparing our NLO predictions with future measurements of $d\Gamma/dx_H$ and $d\Gamma(\uparrow)/dx_H$. One can also test the SM and/or non-SM couplings through polarization measurements involving top-quark decays [mostly $t(\uparrow) \rightarrow b + W^+$]. The formalism made here is also applicable to the production of hadron species other than B and D hadrons, such as pions and kaons, through the polarized top-quark decay using the $b, g \rightarrow \pi/K$ FFs presented in our recent paper [26].

ACKNOWLEDGMENTS

I would like to thank Bernd A. Kniehl and Gustav Kramer for proposing this topic, and I would also like to thank Z. Hamedani for reading and improving the English manuscript.

-
- [1] G. Mahlon and S. J. Parke, *Phys. Rev. D* **55**, 7249 (1997).
 [2] S. Groote, J. G. Körner, B. Melić, and S. Prelovsek, *Phys. Rev. D* **83**, 054018 (2011).
 [3] V. M. Abazov *et al.* (D0 Collaboration), *Phys. Rev. D* **87**, 011103 (2013).
 [4] S. Moch and P. Uwer, *Phys. Rev. D* **78**, 034003 (2008); N. Kidonakis and R. Vogt, *Phys. Rev. D* **78**, 074005 (2008).

- [5] W. Bernreuther, *J. Phys. G* **35**, 083001 (2008).
 [6] N. Cabibbo, *Phys. Rev. Lett.* **10**, 531 (1963); M. Kobayashi and T. Maskawa, *Prog. Theor. Phys.* **49**, 652 (1973).
 [7] B. A. Kniehl, G. Kramer, and S. M. Moosavi Nejad, *Nucl. Phys.* **B862**, 720 (2012).
 [8] S. M. Moosavi Nejad, *Phys. Rev. D* **85**, 054010 (2012); S. M. Moosavi Nejad, *Eur. Phys. J. C* **72**, 2224 (2012).

- [9] A. Ali, F. Barreiro and J. Llorente, *Eur. Phys. J. C* **71**, 1737 (2011).
- [10] B.A. Kniehl, G. Kramer, I. Schienbein, and H. Spiesberger, *Phys. Rev. D* **77**, 014011 (2008).
- [11] T. Kneesch, B. A. Kniehl, G. Kramer, and I. Schienbein, *Nucl. Phys.* **B799**, 34 (2008).
- [12] J. Binnewies, B. A. Kniehl, and G. Kramer, *Phys. Rev. D* **58**, 034016 (1998); M. Cacciari and M. Greco, *Nucl. Phys.* **B421**, 530 (1994).
- [13] C. Caso *et al.* (Particle Data Group Collaboration), *Eur. Phys. J. C* **3**, 1 (1998).
- [14] G. Corcella and A.D. Mitov, *Nucl. Phys.* **B623**, 247 (2002).
- [15] M. Fischer, S. Groote, J.G. Körner, and M.C. Mauser, *Phys. Rev. D* **65**, 054036 (2002).
- [16] M. Fischer, S. Groote, J. G. Körner, M. C. Mauser, and B. Lampe, *Phys. Lett. B* **451**, 406 (1999).
- [17] K. Nakamura (Particle Data Group), *J. Phys. G* **37**, 075021 (2010).
- [18] M. Fischer, S. Groote, J.G. Körner, and M.C. Mauser, *Phys. Rev. D* **63**, 031501 (2001).
- [19] J.C. Collins, *Phys. Rev. D* **58**, 094002 (1998).
- [20] M.G. Bowler, *Z. Phys. C* **11**, 169 (1981).
- [21] V.N. Gribov and L.N. Lipatov, *Yad. Fiz.* **15**, 781 (1972) [*Sov. J. Nucl. Phys.* **15**, 438 (1972)]; G. Altarelli and G. Parisi, *Nucl. Phys.* **B126**, 298 (1977); Yu.L. Dokshitzer, *Zh. Eksp. Teor. Fiz.* **73**, 1216 (1977) [*Sov. Phys. JETP* **46**, 641 (1977)].
- [22] R. Seuster *et al.* (Belle Collaboration), *Phys. Rev. D* **73**, 032002 (2006).
- [23] A. Heister *et al.* (ALEPH Collaboration), *Phys. Lett. B* **512**, 30 (2001).
- [24] G. Abbiendi *et al.* (OPAL Collaboration), *Eur. Phys. J. C* **29**, 463 (2003).
- [25] K. Abe *et al.* (SLD Collaboration), *Phys. Rev. Lett.* **84**, 4300 (2000); *Phys. Rev. D* **65**, 092006 (2002).
- [26] M. Soleymaninia, A. N. Khorramian, S. M. Moosavinejad, and F. Arbabifar, *Phys. Rev. D* **88**, 054019 (2013).